

1,2,3-Oligotriazoles modified halloysite nanotubes as potential active biological species: synthesis and characterization

Marina Massaro,^a Carmelo Giuseppe Colletti,^a Giuseppe Cavallaro,^b Giuseppe Lazzara,^b Paolo Lo Meo,^a Serena Riela,^{*a} and Renato Noto^a

^aDipartimento di Scienze e Tecnologie, Biologiche, Chimiche e Farmaceutiche (STEBICEF), University of Palermo
Viale delle Scienze, Ed. 17 90128 Palermo, Italy

^bDipartimento di Fisica e Chimica "E. Segrè" (DiFC), University of Palermo, Viale delle Scienze, 90128 Palermo,
Italy

Email: serena.riela@unipa.it

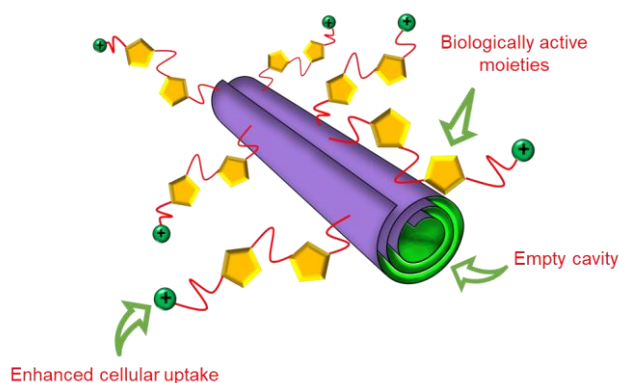
Received 11-04-2021

Accepted Manuscript 01-17-2022

Published on line 01-27-2022

Abstract

In the last years, the development of nano-formulations for cancer treatment represents one of the major challenges of the scientific research. The prodrug strategy, that combines chemotherapeutic agents with nanocarriers such as halloysite nanotubes (HNTs), is a promising strategy both to improve the biological activity of the drug molecules and to reduce the side effects of drugs. Herein we report the synthesis and characterization of a HNTs prodrug based on 1,2,3-triazole units covalently linked to HNTs external surface, bearing different positively charged moieties, which could present interesting pharmacological activities.



HNTs based prodrug system

Keywords: Halloysite nanotubes, 1,2,3-oligotriazole, covalent modification, Huisgen reaction, HNTs-prodrug

Introduction

Nowadays, one of the leading causes of death worldwide is cancer (about 9 million of death for year). The main treatment of the disease is the administration of anticancer agents.¹⁻² However, acute side effects associated to the drug administration and the rapid development of drug resistance hampers the effectiveness of chemotherapy.³ Therefore, there is an urgent need to explore new formulations with low side effects and high efficacy.

An alternative strategy that has attracted interest in the last few years, is the development of suitable carrier systems able to overcome the problem associated to the administration of chemotherapeutic agents. Halloysite nanotubes (HNTs), a clay mineral belonging to the kaolin group, have attracted attention for use in cancer treatment due to their peculiar structure and properties.⁴ HNTs, naturally occurring in massive amount at low cost, show excellent bio-⁵⁻⁷ and ecocompatibility.⁸ Halloysite is positively charged in the inner lumen, which consists mostly of aluminum hydroxide, whereas the external surface, which is silicon dioxide,⁹ is negatively charged. Due to chemical composition, it is possible to selectively modify the HNTs surfaces leading to the development of different nanostructures.¹⁰⁻¹² HNTs have been used as catalysts,¹³⁻¹⁵ materials for pollutant removal,¹⁶⁻¹⁷ fillers for polymeric matrices¹⁸ and often as drug carriers¹⁹⁻²⁰ and delivery systems.²¹⁻²² In this context, one of the most promising feature of HNTs and modified HNTs, is their ability to penetrate the cellular membrane surrounding the cell nuclei.²³⁻²⁴

Heterocyclic compounds represent one of the most important and well-studied branches of medicinal chemistry. The presence of heteroatoms is indeed helpful from a biological point of view, since they may directly affect the reactivity of the target skeleton, the interactions between target drugs and different target inhibitors, the activity (or toxicology) of the compounds, and influence metabolism and pharmacokinetics as well.²⁵⁻²⁶

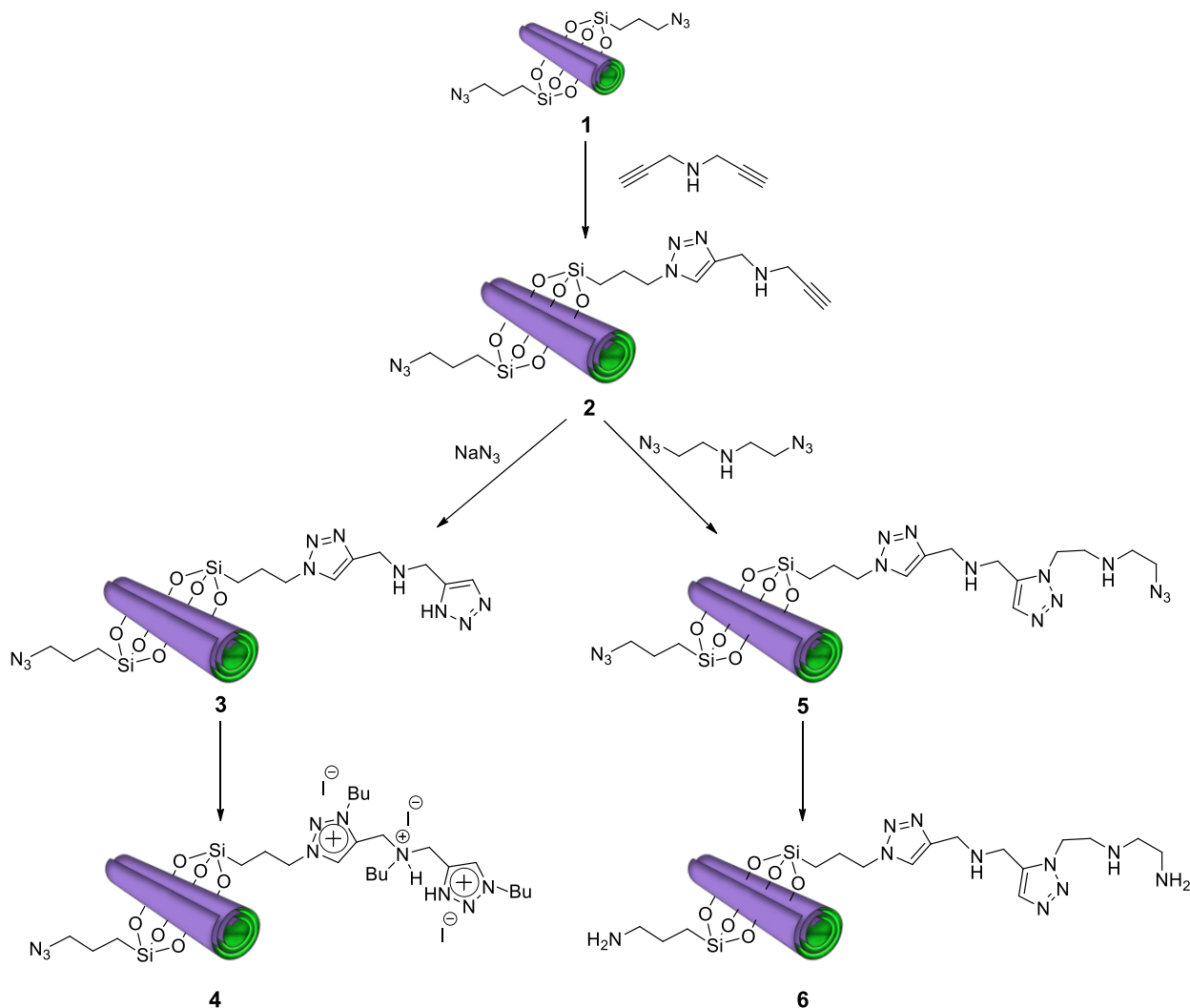
Among the different heterocyclic compounds, promising ones are azoles, five-membered nitrogen heterocycles. The presence of at least two nitrogen heteroatoms in the skeleton offers several advantages in terms of biological interactions. 1,2,3-Triazoles, for example, can form various non-covalent interactions such as hydrophobic interactions, hydrogen bonds, van der Waals forces and dipole-dipole bonds with different biological targets.²⁷ These features provide them and their derivatives with important pharmaceutical properties such as antibacterial, antiviral, anticancer activities and so on.²⁸

In this context, we recently reported the synthesis and characterization of 1,2,3-triazolium salt-modified HNTs as carrier systems for curcumin and cardanol.²⁹⁻³⁰ It was demonstrated that the presence of triazolium salt units in the HNTs carriers allowed for pH-triggered drug release and improved the antitumor effects of both the drugs investigated. Noteworthy, the presence of heterocycles units onto the inorganic carrier exerted synergic effects, thereby increasing the cytotoxic activity of the curcumin and cardanol systems against several tumor cell lines. Therefore, the modification of the HNTs' external surface with triazole units led to the synthesis of "prodrug" system which has showed promising therapeutic activities.

Here we report the synthesis and characterization of a series of modified HNTs bearing different units of 1,2,3-triazole moieties to obtain novel potential prodrug systems for anticancer therapy. The obtained nanomaterials were characterized by FT-IR spectroscopy and thermogravimetric analysis (TGA). The morphology of the systems was also imaged by Scanning Electron Microscopy (SEM) investigations.

Results and Discussion

Halloysite nanotubes prodrug derivatives were synthesized as reported elsewhere,³⁰ by treating HNTs with an excess of 3-azido-propyl trimethoxysilane to afford the nanomaterial **1**. After suitable work-up, the azido groups loading, estimated by thermogravimetric analysis (TGA), was as large as 3.7 wt% with a degree of functionalization of 0.44 mmol g⁻¹. The obtained nanomaterial was used as a building block for a bottom-up synthesis of a series of 1,2,3-oligotriazoles covalently linked onto the HNTs' external surface by means of a copper-catalyzed azido-alkyne cycloaddition (Scheme 1).



Scheme 1. Schematic representation of the synthesis of 1,2,3-oligotriazoles based halloysite nanomaterials.

Firstly, nanomaterial **1** was reacted with dipropargyl amine to give the nanomaterial **2**. The reaction was carried out in a mixture H₂O/^tBuOH (1:1) as solvent, in the presence of catalytic amount of CuSO₄ and sodium ascorbate for 18 h at r.t. to give the nanomaterial **2**. After work-up, we obtained an organic moiety loading of ca. 3 wt% with respect to **1** as estimated by TGA, with a degree of functionalization of 0.32 mmol g⁻¹. Based on the stoichiometric ratio between the nanomaterial **2** and its precursor (**1**), it is possible to conclude that after the cycloaddition reaction some free azido groups are still present on the HNTs' external surface. In

attempting to increase the greenness of the reaction we also carried out the cycloaddition under microwave irradiation, but unfortunately no coupling was achieved.

Afterwards, a first class of nanomaterials was obtained starting from **2**, by reacting it in the presence of sodium azide. In this case, we successfully performed the reaction under MW irradiation at 100 °C, for an irradiation time of 10 min. The latter approach highlights the importance of MW in this kind of synthesis since it significantly reduces the reaction time in comparison to the classical procedure. After work-up, we obtained the nanomaterial **3** with a percent loading of organic moiety of 2.5 wt% with respect to nanomaterial **2**. Since previous studies on the biological properties of triazolium salt-modified HNTs highlighted the importance of a positive charge on the heterocycle ring, both for the controlled release of a drug and to improve the pharmacological activity of systems, we further modified **3** by reaction with butyl iodide to obtain the nanomaterial **4**.

Nanomaterial **2** was also reacted with bis (2-azidoethyl) amide to afford the nanomaterial **5**. The reaction was carried out in a mixture of H₂O/*t*BuOH (1:1) as solvent, in the presence of catalytic amount of CuSO₄ and sodium ascorbate for 18 h at r.t. The loading percent of organic moiety was estimated by TGA as large as 1 wt% with a degree of functionalization of 0.06 mmol g⁻¹. The low loading obtained in this case led us to conclude that several -N₃ groups are still present onto HNTs' surface, and that they could still be able to undergo further functionalization. The nanomaterial **5** was then subjected to post-modification by reduction under the Staudinger reaction conditions (triphenylphosphine, DMF, r.t.) to obtain nanomaterial **6** (Scheme 1). The post-modification step was crucial since in this way free amino groups were introduced onto the prodrug systems which could be important for nanomaterial internalization and therefore for cellular uptake.²⁴

The synthesized nanomaterials were characterized by FT-IR spectroscopy and thermogravimetric analysis. In Figure 2 are reported the FT-IR spectra of the final nanomaterials **4** and **6** within their precursor **2**. Compared to the FT-IR spectra of **1**, the FT-IR spectra of the nanomaterials **4** and **6** exhibit the typical vibration stretching bands of precursor with some variations. Besides the typical HNTs vibration peaks, the FT-IR spectrum of both **4** and **6** shows the vibration stretching bands for C-H stretching of methylene groups at ca. 2960 and 2865 cm⁻¹. Furthermore, some peaks in the range 1583, 1400 cm⁻¹, due to the vibration stretching bands of heterocycle rings, can be observed. It is noteworthy that in the FT-IR spectrum of **4** an intense signal at ca. 2100 cm⁻¹ is still visible, due to the presence of the unreacted excess of azido groups (Figure 2a). Conversely, after reduction of the azido groups by means of PPh₃, the FT-IR spectrum of nanomaterial **6** exhibits the almost complete disappearance of the N₃ vibration band (Figure 2b). All these features confirm the synthesis of 1,2,3-oligotriazole based halloysite nanomaterials.

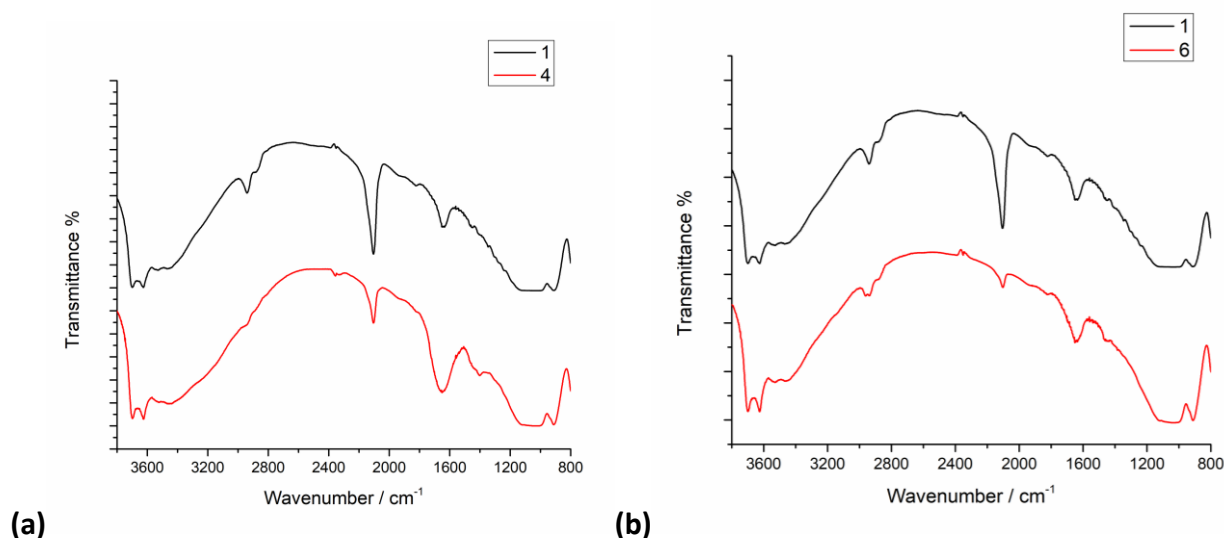


Figure 2. FT-IR spectra of the nanomaterials **1**, **4** and **6**.

As stated above, the 1,2,3-triazole amount grafted onto the HNTs was estimated by TGA. TGA data confirmed the successful functionalization of HNTs' external surface after each synthetic step. In the thermoanalytical curves of the final nanomaterials, beside the typical mass loss of HNTs at ca. 500 °C due to the to the expulsion of interlayer water molecules, are indeed, present additional mass losses in the range 200-300 °C which are attributable to the organic moieties grafted (Figure 3).

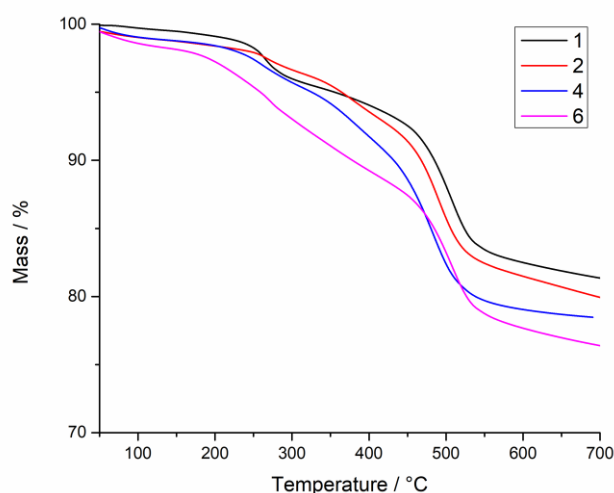


Figure 3. Thermoanalytical curves of the nanomaterials **1**, **2**, **4** and **6**.

In the last years the use of scanning electron microscopy (SEM) to investigate the morphology of HNTs based nanomaterials has attracted attention due to the information which can be obtained by this technique.³¹ Therefore, we imaged the surface morphology of the nanomaterials **4** and **6** by SEM (Figure 4). As it is possible to note, the tubular shape of the halloysite is maintained after the cycloaddition reaction. Furthermore, conversely to the SEM image of pristine HNTs,³² the micrographies of the synthesized

nanomaterials show a rather compact structure in both nanomaterials, where nanotubes seem to be glued together because of interactions established by the organic structures grafted on the external surface.

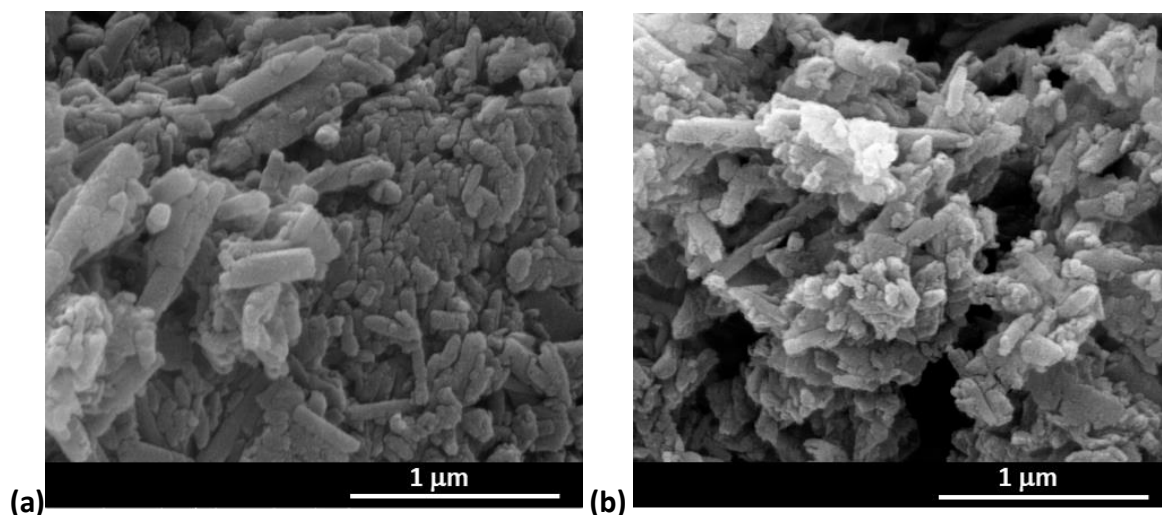


Figure 4. SEM of nanomaterial (a) **4** and (b) **6**.

Conclusions

Halloysite nanotubes bearing 1,2,3-triazolium salt derivatives were developed as a suitable carrier system with the aim of eventually enhancing both the therapeutic effect of the drug and increasing cellular uptake. The success of the synthetic strategies adopted was highlighted by thermogravimetric analysis and all nanomaterials were characterized by FT-IR spectroscopy and their morphology was imaged by SEM investigations. The HNT nanomaterials obtained in this research could be promising for future investigations into prodrug strategies to be evaluated by means of *in vitro* studies.

Experimental Section

General. All reagents were purchased from Sigma-Aldrich by Merck and used without further purification. Nanomaterial **1** and bis (2-azidoethyl) amine were prepared as reported in literature.^{30, 33} Microwave-assisted syntheses were carried out with a CEM DISCOVER monomode system in a closed vessel. Thermogravimetric analyses were performed on a Q5000 IR apparatus (TGA Instruments) under a nitrogen flow of 25 cm³ min⁻¹ for the sample and 10 cm³ min⁻¹ for the balance. The weight of each sample was ca. 5 mg. Measurements were carried out by heating the sample from room temperature up to 900 °C at a rate of 10 °C min⁻¹. IR spectra (KBr) were recorded with an Agilent Technologies Cary 630 FT-IR spectrometer. Specimens for these measurements were prepared by mixing 5 mg of the sample powder with 100 mg of KBr. An ESEM FEI QUANTA 200 F microscope was used to study the morphology of the functionalized Hal. Before each experiment, the sample was coated with gold under argon by means of an Edwards Sputter Coater S150A to avoid charging under the electron beam.

Synthesis of nanomaterial 2. To a dispersion of **1** (300 mg) in H₂O/^tBuOH (1:1) mixture (3 mL) dipropargyl amine (20 mL, 1.5 eq) was added. The mixture was stirred under argon in the presence of catalytic amount of CuSO₄/sodium ascorbate solution (1 M, 1:10 v/v) at room temperature for 18 h. After this time, the solvent was filtered off, the powder was rinsed with H₂O, then with MeOH and finally dried at 80 °C under vacuum.

Percent loading: 3 wt%

Degree of functionalization: 0.32 mmol g⁻¹.

Synthesis of nanomaterial 3. Nanomaterial **2** (50 mg), NaN₃ (15 mg, 0.23 mmol), 1 mg of CuSO₄ × 5H₂O and 1.5 mg of sodium ascorbate were weighed in a microwave test tube provided with a cup. Afterwards, 1 mL of a mixture H₂O/^tBuOH (1:1) was added and the dispersion was subjected to ultrasound (200 W) for ca. 1 min. The crude was inserted in the MW apparatus at 100 °C, under constant stirring, for 10 min. Successively, the solid was collected by centrifuge, washed three times with water and three times with CH₂Cl₂ and finally dried at 60 °C under vacuum.

Percent loading: 2.5 wt%

Degree of functionalization: 0.38 mmol g⁻¹.

Synthesis of nanomaterial 4. To a dispersion of **3** (50 mg) in dry toluene (5 mL) and an excess of the 1-iodobutane (620 mL, 5.4 mmol) was added. The suspension was then refluxed at 120 °C for 24 h. After this time, the solid was filtered off, rinsed with CH₃OH and CH₂Cl₂ and finally dried at 60 °C under vacuum.

Synthesis of nanomaterial 5. To a dispersion of **2** (200 mg) in H₂O/^tBuOH (1:1) mixture (4 mL), bis(2-azidoethyl) amine (40 mg, 0.26 mmol) was added. The mixture was stirred under argon in the presence of catalytic amount of CuSO₄/sodium ascorbate solution (1 M, 1:10 v/v) at room temperature for 18 h. After this time, the solvent was filtered off, the powder was rinsed with H₂O, then with MeOH and finally dried at 80 °C under vacuum.

Percent loading: 1 wt%

Degree of functionalization: 0.06 mmol g⁻¹.

Synthesis of nanomaterial 6. To a dispersion of **5** (50 mg) in DMF (2 mL) and triphenylphosphine (PPh₃) (30 mg, 0.11 mmol) was added to the reaction mixture under inert atmosphere. The dispersion was left to stir at room temperature for 1 h. After this time a NH₃ aqueous solution (150 μL) was added dropwise. After 4 days the solvent was filtered off and the powder was washed several times with water and CH₂Cl₂ and finally dried at 50 °C under vacuum.

Percent loading: 1 wt%

Degree of functionalization: 0.0.6 mmol g⁻¹.

Acknowledgements

The work was financially supported by the University of Palermo.

References

1. Islam, M. S.; Wang, C.; Zheng, J.; Paudyal, N.; Zhu, Y.; Sun, H., *Eur. J. Med. Chem.* **2019**, *162*, 109-121. <https://doi.org/10.1016/j.ejmech.2018.11.001>
2. Zhang, J.; Wang, S.; Ba, Y.; Xu, Z., *Eur. J. Med. Chem.* **2019**, *178*, 341-351. <https://doi.org/10.1016/j.ejmech.2019.05.071>

3. Ammar, U. M.; Abdel-Maksoud, M. S.; Oh, C.-H., *Eur. J. Med. Chem.* **2018**, *158*, 144-166.
<https://doi.org/10.1016/j.ejmech.2018.09.005>
4. Liu, M.; Jia, Z.; Jia, D.; Zhou, C., *Prog. Polym. Sci.* **2014**, *39* (8), 1498-1525.
<https://doi.org/10.1016/j.progpolymsci.2014.04.004>
5. Fakhru'llina, G. I.; Akhatova, F. S.; Lvov, Y. M.; Fakhru'llin, R. F., *Environm. Sci. Nano* **2015**, *2* (1), 54-59.
<https://doi.org/10.1039/C4EN00135D>
6. Kryuchkova, M.; Danilushkina, A.; Lvov, Y.; Fakhru'llin, R., *Environm. Sci. Nano* **2016**, *3* (2), 442-452.
<https://doi.org/10.1039/C5EN00201J>
7. Rozhina, E.; Ishmuhametov, I.; Batasheva, S.; Fakhru'llin, R., *BioNanoScience* **2018**, *8* (1), 310-312.
<https://doi.org/10.1007/s12668-017-0453-8>
8. Bellani, L.; Giorgetti, L.; Riela, S.; Lazzara, G.; Scialabba, A.; Massaro, M., *Environ. Toxicol. Chem.* **2016**, *35* (10), 2503-2510.
<https://doi.org/10.1002/etc.3412>
9. Bretti, C.; Cataldo, S.; Gianguzza, A.; Lando, G.; Lazzara, G.; Pettignano, A.; Sammartano, S., *J. Phys. Chem. C* **2016**, *120* (14), 7849-7859.
<https://doi.org/10.1021/acs.jpcc.6b01127>
10. Stavitskaya, A. V.; Novikov, A. A.; Kotelev, M. S.; Kopitsyn, D. S.; Rozhina, E. V.; Ishmukhametov, I. R.; Fakhru'llin, R. F.; Ivanov, E. V.; Lvov, Y. M.; Vinokurov, V. A., *Nanomaterials* **2018**, *8* (6), 391.
<https://doi.org/10.3390/nano8060391>
11. Massaro, M.; Noto, R.; Riela, S., *Molecules* **2020**, *25* (20). 10.3390/molecules25204863.
<https://doi.org/10.3390/molecules25204863>
12. Peixoto, D.; Pereira, I.; Pereira-Silva, M.; Veiga, F.; Hamblin, M. R.; Lvov, Y.; Liu, M.; Paiva-Santos, A. C., *Coord. Chem. Rev.* **2021**, *440*, 213956.
<https://doi.org/10.1016/j.ccr.2021.213956>
13. Massaro, M.; Casiello, M.; D'Accolti, L.; Lazzara, G.; Nacci, A.; Nicotra, G.; Noto, R.; Pettignano, A.; Spinella, C.; Riela, S., *Appl. Clay Sci.* **2020**, *189*.
<https://doi.org/10.1016/j.clay.2020.105527>
14. Lin, T.; Zhao, S.; Niu, S.; Lyu, Z.; Han, K.; Hu, X., *Energy Convers. Manage.* **2020**, *220*.
<https://doi.org/10.1016/j.enconman.2020.113138>
15. Stavitskaya, A. V.; Kozlova, E. A.; Kurenkova, A. Y.; Glotov, A. P.; Selischev, D. S.; Ivanov, E. V.; Kozlov, D. V.; Vinokurov, V. A.; Fakhru'llin, R. F.; Lvov, Y. M., *Chem. Eur. J.* **2020**, *26* (57), 13085-13092.
<https://doi.org/10.1002/chem.202002192>
16. Massaro, M.; Riela, S.; Cavallaro, G.; Colletti, C. G.; Milioto, S.; Noto, R.; Lazzara, G., *ChemistrySelect* **2016**, *1* (8), 1773-1779.
<https://doi.org/10.1002/slct.201600322>
17. Salaa, F.; Bendenia, S.; Lecomte-Nana, G. L.; Khelifa, A., *Chem. Eng. J.* **2020**, *396*.
<https://doi.org/10.1016/j.cej.2020.125226>
18. Naumenko, E.; Guryanov, I.; Zakirova, E.; Fakhru'llin, R., *Polymers* **2021**, *13* (22), 3949.
<https://doi.org/10.3390/polym13223949>
19. Massaro, M.; Poma, P.; Colletti, C. G.; Barattucci, A.; Bonaccorsi, P. M.; Lazzara, G.; Nicotra, G.; Parisi, F.; Salerno, T. M. G.; Spinella, C.; Riela, S., *Appl. Clay Sci.* **2020**, *184*.
<https://doi.org/10.1016/j.clay.2019.105400>
20. Massaro, M.; Buscemi, G.; Arista, L.; Biddeci, G.; Cavallaro, G.; D'Anna, F.; Di Blasi, F.; Ferrante, A.; Lazzara, G.; Rizzo, C.; Spinelli, G.; Ullrich, T.; Riela, S., *ACS Med. Chem. Lett.* **2019**, *10* (4), 419-424.

<https://doi.org/10.1021/acsmchemlett.8b00465>

21. Alfieri, M. L.; Massaro, M.; d'Ischia, M.; D'Errico, G.; Gallucci, N.; Gruttadauria, M.; Licciardi, M.; Liotta, L. F.; Nicotra, G.; Sfuncia, G.; Riela, S., *J. Colloid Interface Sci.* **2022**, *606*, 1779-1791.

<https://doi.org/10.1016/j.jcis.2021.08.155>

22. Massaro, M.; Riela, S.; Baiamonte, C.; Blanco, J. L. J.; Giordano, C.; Lo Meo, P.; Milioto, S.; Noto, R.; Parisi, F.; Pizzolanti, G.; Lazzara, G., *RSC Adv.* **2016**, *6* (91), 87935-87944.

<https://doi.org/10.1039/C6RA14657K>

23. Lvov, Y.; Aerov, A.; Fakhrullin, R., *Adv. Colloid Interface Sci.* **2014**, *207*, 189-198.

<https://doi.org/10.1016/j.cis.2013.10.006>

24. Massaro, M.; Barone, G.; Biddeci, G.; Cavallaro, G.; Di Blasi, F.; Lazzara, G.; Nicotra, G.; Spinella, C.; Spinelli, G.; Riela, S., *J. Colloid Interface Sci.* **2019**, *552*, 236-246.

<https://doi.org/10.1016/j.jcis.2019.05.062>

25. Ayati, A.; Emami, S.; Foroumadi, A., *Eur. J. Med. Chem.* **2016**, *109*, 380-392.

<https://doi.org/10.1016/j.ejmech.2016.01.009>

26. Abdellatif, K. R. A.; Bakr, R. B., *Bioorg. Chem.* **2018**, *78*, 341-357.

<https://doi.org/10.1016/j.bioorg.2018.03.032>

27. Xu, Z.; Zhao, S.-J.; Liu, Y., *Eur. J. Med. Chem.* **2019**, *183*, 111700.

<https://doi.org/10.1016/j.ejmech.2019.111700>

28. Zhang, B., *Eur. J. Med. Chem.* **2019**, *168*, 357-372.

<https://doi.org/10.1016/j.ejmech.2019.02.055>

29. Massaro, M.; Colletti, C. G.; Noto, R.; Riela, S.; Poma, P.; Guernelli, S.; Parisi, F.; Milioto, S.; Lazzara, G., *Int. J. Pharm.* **2015**, *478* (2), 476-485.

<https://doi.org/10.1016/j.ijpharm.2014.12.004>

30. Riela, S.; Massaro, M.; Colletti, C. G.; Bommarito, A.; Giordano, C.; Milioto, S.; Noto, R.; Poma, P.; Lazzara, G., *Int. J. Pharm.* **2014**, *475* (1), 613-623.

<https://doi.org/10.1016/j.ijpharm.2014.09.019>

31. Cherednichenko, K.; Kopitsyn, D.; Batasheva, S.; Fakhrullin, R., *Polymers* **2021**, *13* (20), 3510.

<https://doi.org/10.3390/polym13203510>

32. Massaro, M.; Barone, G.; Barra, V.; Cancemi, P.; Di Leonardo, A.; Grossi, G.; Lo Celso, F.; Schenone, S.; Viseras Iborra, C.; Riela, S., *Int. J. Pharm.* **2021**, *599*, 120281.

<https://doi.org/10.1016/j.ijpharm.2021.120281>

33. Song, Y.; Zong, H.; Trivedi, E. R.; Vesper, B. J.; Waters, E. A.; Barrett, A. G. M.; Radosevich, J. A.; Hoffman, B. M.; Meade, T. J., *Bioconjugate Chem.* **2010**, *21* (12), 2267-2275.

<https://doi.org/10.1021/bc1002828>

This paper is an open access article distributed under the terms of the Creative Commons Attribution (CC BY) license (<http://creativecommons.org/licenses/by/4.0/>)